

Measuring the effect of shuttles on the overall efficiency of a slipper type axial piston pump

Peter Achten, Robin Mommers and Jeroen Potma

INNAS BV, Nikkelstraat 15, 4823 AE Breda, the Netherlands
E-Mail: pachten@innas.com

Part of the losses of hydrostatic machines are commutation losses, sometimes also called compression losses. These losses are caused by the unavoidable and continuous process of compressing and expanding oil in the displacement chambers of a pump or motor. The commutation losses are strongly pressure related, but also depend on other factors like the bulk modulus of the oil, the amount of dead volume and the design and sizing of any silencing grooves. Depending on the operating conditions, commutation losses can amount to 50% of the total losses of a pump [1].

Shuttles are a means to reduce or maybe even eliminate these losses. Shuttles are small connections between the individual and neighbouring cylinders or displacement chambers. Inside each of these connections, there is a ball, which acts as a valve body in the extreme positions, and acts as a displacer when moving from one seat to the other. Shuttles have been introduced for the first time in hydraulic transformers [2]. In 2021, a solution was presented for applying shuttles in pumps and motors [3].

This paper will present the experimental results of testing shuttles in a 28 cc fixed displacement slipper type pump from Rexroth (A4FO28), which was tested with and without shuttles. The experimental results are presented and compared in this paper. Adding shuttles to the pump has increased the peak efficiency from 91,9 to 96,4%. In the range between 500 and 3000 rpm, and between 100 and 400 bar, the average overall efficiency has increased from 90,8% to 94,3%.

Keywords: hydraulic pumps, efficiency, commutation losses, shuttles

Target audience: Hydraulic pump and motor developers and industry,

1. Introduction

Hydrostatic pumps operate between two pressure levels: a low pressure level at the supply side, and a high pressure level at the delivery side of the pump. As an example, a nine piston axial piston pump switches 18 times per revolution from one pressure level to the other: from low to high pressure in the bottom dead centre (BDC) and from high to low pressure in the top dead centre (TDC). At a rotational speed of 3000 rpm, this amounts to 900 switches per second.

This switching process is called commutation. It not only occurs in hydrostatic pumps, but also in motors and hydraulic transformers, in both fixed and variable displacement machines. There are a few pumps which use valves to facilitate and enable the switching process, but the vast majority of hydrostatic machines uses a distributor, similar to the function of a commutator in direct current electric machines with brushes. In axial piston machines, the valve plate or port plate acts as the distributor. Similar devices can be found in radial piston pumps and motors, in vane pumps, in gerotor and geroler motors, and even in gear pumps.

In an ideal machine, for example in an ideal axial piston pump, oil is compressed and expanded by means of the piston movement. For instance in the BDC, the piston and its cylinder move from the low pressure kidney of the valve plate to the high pressure kidney. In between these two kidneys is the sealing land. When the barrel port is closed off by the sealing land, it has (for a short time) no connection to either the low or the high pressure side of

the pump. In that case, the ongoing piston movement will result in a compression of the oil inside its cylinder, since the barrel port of the cylinder is closed by the sealing land,

In this imaginary ideal pump, the sealing land around the BDC needs to be dimensioned as such, that the compression stops precisely at the moment, when the pressure level in the barrel cylinder reaches the pressure level of the high pressure kidney. If the sealing land is too short, the compression will not be enough, and the oil in the cylinder will open up too soon to the high pressure kidney. If the sealing land is too long, high pressure spikes will occur. Also in the commutation zone of the TDC, the sealing land needs to be dimensioned exactly right (i.e. not too long and not too short) in order to avoid short circuiting or cavitation.

The problem is that the geometry and dimensions of the valve plate are fixed after production, whereas the 'ideal' timing of the commutation cannot be defined as a constant. The amount of compression and expansion strongly depends on parameters like the pump pressure, the bulk modulus of the oil, the amount of leakage (and hence the oil temperature) and even the rotational speed of the pump. In current pumps and motors, a compromise solution has been found in accepting that the commutation can't be ideal. Instead, most commutation conflicts are softened by means of silencing grooves or pressure relief grooves.

The design of the valve plate and its silencing grooves has been a subject of many studies in the past. The design determines the noise, pressure pulsations, torque variations, and compression and expansion losses. Commutation often results in substantial losses. Kuipers [4] and Douma and Ottens [5] were one of the first to write about commutation losses. According to these early publications, the overall efficiency of pumps could be increased by up to 2%. In 2021, INNAS published a methodology to determine the commutation losses [1]. By means of variation of the dead volume, the effect of the commutation losses on the overall efficiency could be measured for a 23,7 cc fixed displacement floating cup pump. At a pump pressure of 400 bar and a rotational speed of 4500 rpm, the commutation losses had an impact of 50% of the total losses.

In order to reduce the commutation losses, attempts have been made to reduce the amount of dead volume. In slipper type pumps and motors, the pistons are often made hollow to reduce the centrifugal forces and the barrel tipping torque, especially in variable displacement machines. However, this creates a larger dead volume and therefore increases the commutation losses. A possible compromise solution would be to close the piston cavity at the end, thereby creating a hollow and relatively light piston, but without an increase of the dead volume [6].

In variable displacement machines, several mechanisms or linkages have been suggested which reduce the cylinder volume, when the displacement of the machine has reduced [7-9]. In conventional variable displacement machines, the cylinder volume has reduced at smaller displacements, at least in and around the bottom dead center, but at the same time the volume has increased during the commutation around the top dead center. The proposed mechanical solutions are designed to reduce the cylinder volume in both dead centers, thus reducing the losses due to commutation.

Other design concepts to improve the commutation are:

- the use of a precompression filter volume (PCFV) [10];
- a decompression filter volume (DCFV) possibly combined with PCFV [11];
- the use of check valves [12, 13];
- so called cross angle designs of axial piston pumps [14, 15];
- the use of an indexing valve plate with a controlled rotational position of the valve plate [16].

Most of these concepts were meant to reduce the noise level of pumps, not the power losses. Furthermore, most designs were aimed at (slipper type) axial piston pumps.

In 2021, INNAS presented a more general solution for applying shuttles in hydrostatic pumps and motors [3]. Shuttles can, in theory, completely eliminate the commutation losses, thereby strongly increasing the overall efficiency. The solution can be applied in any hydrostatic machine which uses a distributor or valve plate. The solution is applicable for both fixed and variable displacement machines.

In this paper, the shuttle solution is described for a 28 cc fixed displacement axial piston pump from Bosch Rexroth (A4FO28/32R). This pump is tested with and without shuttles, in a wide range of operating conditions. This paper describes the results of this empirical study: the effects of the use of shuttles on the overall efficiency,

the drain leakage and the total losses, the hydromechanical losses and the volumetric losses. The tests were performed at INNAS. The test bench has been described in [17]. The efficiencies and losses, as presented in this paper, are defined in [18].

2. Construction details

In order to measure the effects of the shuttles, the pump has been tested first as a standard pump, without any adaptations and without shuttles being applied. After that, the pump was adapted for allowing shuttles to be used:

- Connections i.e. shuttle cylinders were made between each pair of neighbouring barrel cylinders;
- A new valve plate was designed and manufactured, without silencing grooves but with larger sealing lands;
- After the production of the new port plate, the spherical bearing surfaces of the port plate and the barrel were lapped together in order to match both surface profiles.

Aside from the new valve plate and the adaptation of the barrel, all other components have been kept the same: the housing, the pistons, the cylinders, the slippers and the other components of the rotating group, such as the bearings, the shaft, the shaft seal and the barrel springs all remained the same. This way, any effects measured can only be attributed to the shuttles and the new valve plate.

2.1. Applying shuttles in the barrels

Fitting the shuttles into the design of the existing barrel was a challenge. Evidently, the original A4FO28 [19] is not designed for having shuttles applied. As is described in [3], the shuttles need to be positioned in a certain way in order to use the pressure difference across the barrel ports. Furthermore, the shuttle volume needed to be large enough for any pump operation between 0 and 400 bar. Finally, the shuttles must be positioned as such that the centrifugal forces don't influence the movement and positioning of the shuttle balls.

The design of the adapted barrel has also been made as such, that the shuttles could be altered, allowing to change the size of the shuttle balls or to apply balls with a different material and mass. These constraints created some difficulties in fitting the shuttles inside the existing barrel designs. It resulted in a compromise solution, in which one end of the shuttles has a 90° angled connection to the cylinder, which results in a larger flow restriction and thus in higher pressure differences than preferable.

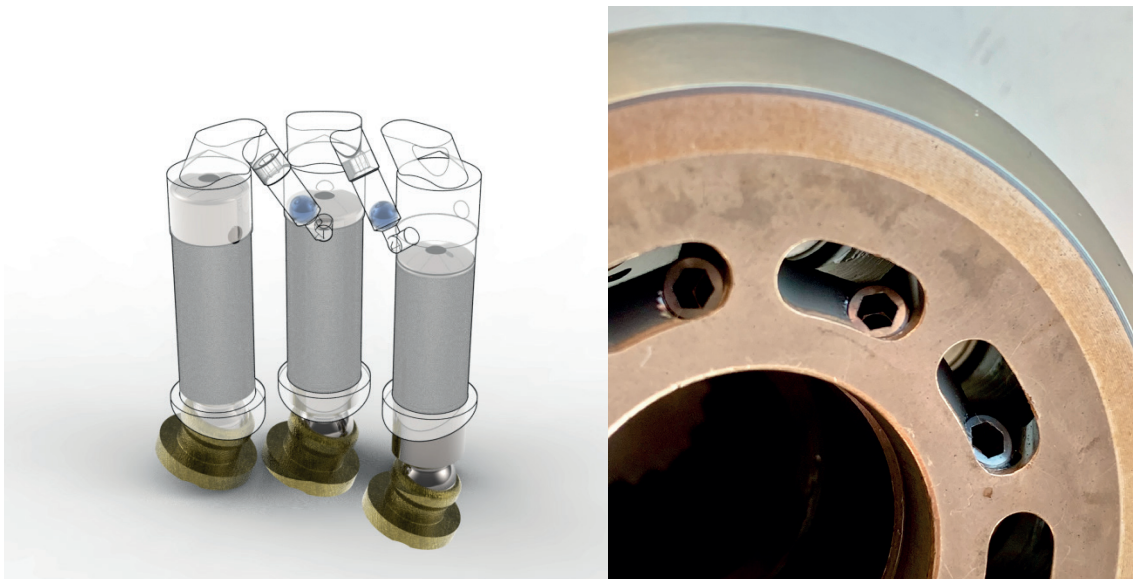


Fig. 1: Shuttles in the barrel of the A4FO28-pump. The drawing on the left shows three of the nine pistons and cylinders. Each cylinder is connected to two shuttles, as is shown for the middle cylinder. In total, there are nine shuttles applied. The photo on the right shows the hollow plugs which were mounted via the existing barrel ports.

Each barrel cylinder is connected to two shuttles: one leading (in the direction of rotation of the barrel) and one following. The shuttle-balls are ceramic balls with a diameter of 4,5 mm and a mass of 0,37 gram. The shuttle chamber has a diameter of 4,9 mm. The shuttle balls make a stroke of 6 mm inside the shuttle cylinder. In the end positions, the shuttles act as a check valve, having the shuttle balls pushed into a conical seat. It is not necessary to have a tight fit between the shuttle ball and its cylinder. In this example, the diameter difference is 0,4 mm.

2.2. New valve plate

A new valve plate design is needed when shuttles are mounted in the barrel. Figure 2 shows the old and the new design of the valve plate. The new valve plate does not rely on silencing grooves anymore. Instead, the sealing lands around the top and bottom dead centres (TDC and BDC) are increased. The length of the sealing lands is determined by the maximum pump pressure and should be at least large enough to allow for a full compression (after the BDC) and full expansion (after the TDC). The sealing lands may even be larger, as long as the shuttles are large enough to compensate for any differences or mismatches.

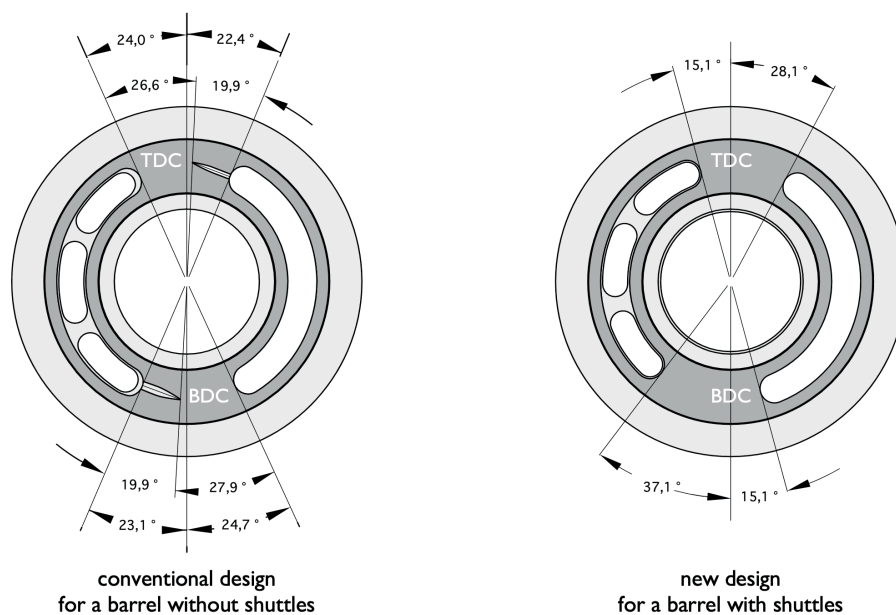


Fig. 2: Old and new design of the A4FO28 valve plates

The barrel ports, which move across the port plate, have an arc length of $30,2^\circ$. In the new valve plate design, the sealing lands have a length of $15,1 + 28,1 = 43,2^\circ$ in the TDC and of $15,1 + 37,1 = 52,2^\circ$ in the BDC. This is much larger than the arc length of the barrel port. The difference is used to allow for a full compression and expansion of the oil in the barrel cylinder, even when the pump is operated at maximum pressure. The distance between the end of the low pressure kidney and the BDC, and between the end of the high pressure kidney and the TDC is $15,1^\circ$, which is half the arc length of the barrel port. Consequently, the barrel ports close exactly at the TDC and BDC positions of the pistons. Immediately after having reached one of the two dead centers, the piston movement starts the compression (BDC) or expansion (TDC) of the oil contents of the cylinder.

If the pump is operated at a lower pressure than the maximum pump pressure, the compression or expansion will stop after the pressure in the barrel cylinder has reached the pressure level of the next kidney. At that point, the shuttle ball of the leading shuttle will start to move, thus avoiding any overpressure or cavitation.

Contrary to the positive overlap of the new valve plate, the old valve plate has a negative overlap with respect to the silencing grooves. Consequently, there is some degree of short-circuiting. Furthermore, the barrel ports are immediately connected to the next kidney, which results in an extremely fast compression or expansion with high pressure change rates. The silencing grooves limit these rates to some extent, but nevertheless the rates are very high, resulting not only in dissipative losses across the silencing grooves, but also in strong pressure and flow pulsations, noise and possibly cavitation and wear.

3. Test procedure

The pump was tested at INNAS following the pump specifications of Bosch Rexroth [19]. Details about the test bench and test procedure can be found in [17, 20]. A list of sensors and their specification can be found in Appendix A. All tests have been performed with Shell Tellus Oil S2 MX46 at an oil supply temperature of 50°C ($\pm 0,5^\circ\text{C}$). In order to measure at a maximum allowable rotational speed of 3750 rpm, the supply pressure needed to be 1 bar above atmospheric pressure [19]. Efficiencies and losses are defined according to [18]. The A4FO28 has been tested in 104 different operating points, ranging between 50 and 400 bar and between 10 and 3750 rpm (see Table 1).

Table 1: Measured operating points of the A4FO28. In the points indicated with \checkmark^* an additional supply pump was needed for the original A4FO28 to overcome the leakage. In the points indicated with \checkmark^{**} an additional supply pump was needed for both the original and the adapted A4FO28 to overcome the leakage

	pump pressure p_2							
	50 bar	100 bar	150 bar	200 bar	250 bar	300 bar	350 bar	400 bar
10 rpm	\checkmark^{**}	\checkmark^{**}	\checkmark^{**}	\checkmark^{**}	\checkmark^{**}	\checkmark^{**}	\checkmark^{**}	\checkmark^{**}
25 rpm	\checkmark	\checkmark^*	\checkmark^*	\checkmark^{**}	\checkmark^{**}	\checkmark^{**}	\checkmark^{**}	\checkmark^{**}
50 rpm	\checkmark	\checkmark	\checkmark	\checkmark	\checkmark	\checkmark	\checkmark^*	\checkmark^*
100 rpm	\checkmark	\checkmark	\checkmark	\checkmark	\checkmark	\checkmark	\checkmark	\checkmark
250 rpm	\checkmark	\checkmark	\checkmark	\checkmark	\checkmark	\checkmark	\checkmark	\checkmark
500 rpm	\checkmark	\checkmark	\checkmark	\checkmark	\checkmark	\checkmark	\checkmark	\checkmark
1000 rpm	\checkmark	\checkmark	\checkmark	\checkmark	\checkmark	\checkmark	\checkmark	\checkmark
1500 rpm	\checkmark	\checkmark	\checkmark	\checkmark	\checkmark	\checkmark	\checkmark	\checkmark
2000 rpm	\checkmark	\checkmark	\checkmark	\checkmark	\checkmark	\checkmark	\checkmark	\checkmark
2500 rpm	\checkmark	\checkmark	\checkmark	\checkmark	\checkmark	\checkmark	\checkmark	\checkmark
3000 rpm	\checkmark	\checkmark	\checkmark	\checkmark	\checkmark	\checkmark	\checkmark	\checkmark
3500 rpm	\checkmark	\checkmark	\checkmark	\checkmark	\checkmark	\checkmark	\checkmark	\checkmark
3750 rpm	\checkmark	\checkmark	\checkmark	\checkmark	\checkmark	\checkmark	\checkmark	\checkmark

All operating points are measured at steady state conditions for a period of 10 seconds with 0,05 seconds interval between the individual measurement points. These data are averaged in post-processing. The pump was provided with an external drain which allows for the measurement of the drain leakage from the case. Before each test cycle, a running-in procedure was performed for the pump, for the original and the adapted pump.

At low rotational speeds, the leakage of the pump can become larger than the flow that the pump can deliver. In those cases, the pump is not capable of maintaining the desired pump pressure, and an additional supply pump is used to maintain the desired pressure level. When the additional supply pump is operated, it is no longer possible to measure and define the overall efficiency. In Table 1, these points are indicated by * or **.

4. Test results

4.1 Overall efficiency and total power losses

Shuttles and the complementary new valve plate have significantly improved the performance of the pump (Table 2). The peak efficiency has been increased from 91,9% to 96,4%. In the range between 500 and 3000 rpm, and 100 and 400 bar, the average overall efficiency has increased from 90,8% to 94,3%. The overall losses are reduced on average by 41%. The contour plots of Figure 3 show the measured overall efficiency of the A4FO28, without shuttles (left diagram, Fig. 3a) and with shuttles (right diagram, Fig 3b).

Table 2: Main effects of the shuttles on the overall efficiency and losses

	without shuttles	with shuttles	improvement
peak efficiency	91,9%	96,4%	4,5%-points higher efficiency
average* efficiency	90,8%	94,3%	3,5%-points higher efficiency
average* overall power loss [kW]	1,93	1,14	0,79 kW or 41,0 % reduction

*500 ≤ n ≤ 3000 rpm, 100 ≤ p₂ ≤ 400 bar

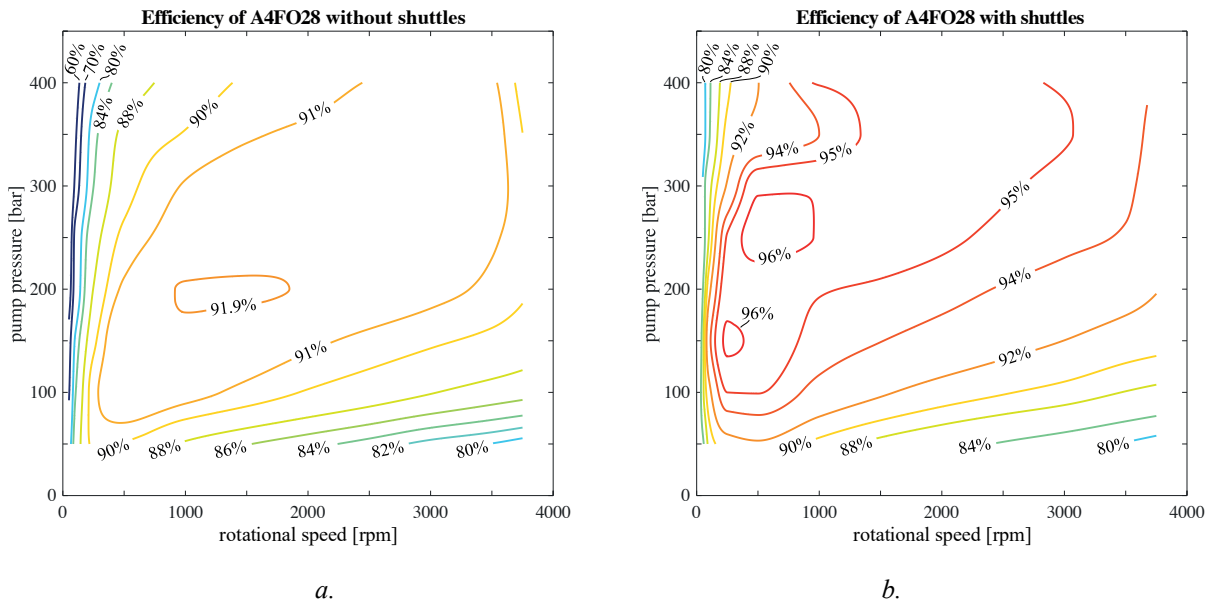


Fig. 3: Overall efficiency of the A4FO28 with (a) and without (b) shuttles applied

The contour plot of Figure 4a shows how much the overall efficiency has increased in each point when shuttles are applied. Appendix B includes two tables with the measured test results. Only at 50 bar and high rotational speeds ($n \geq 3500$ rpm), there is no improvement of the overall efficiency. In all other points the overall efficiency has increased, especially at pump pressures above 200 bar. This is also expected. The shuttles reduce the commutation losses, which are strongly pressure dependent.

In addition, the right diagram of Figure 4 (Fig. 4b) shows the relative reduction of the total power losses:

$$\frac{P_{loss,tot,without} - P_{loss,tot,with}}{P_{loss,tot,without}} \quad (1)$$

The subindexes ‘with’ and ‘without’ refer to the pump with or without the shuttles. The shuttles strongly reduce the overall losses of the pump and create a significant increase of the overall efficiency.

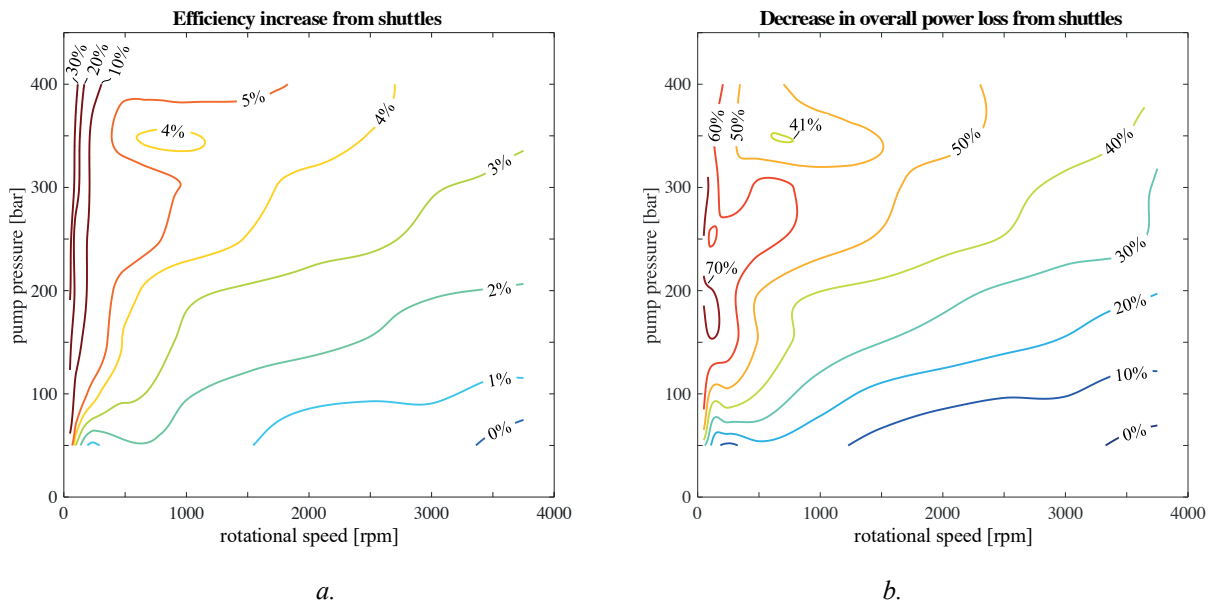


Fig. 4: Measured reduction of the overall efficiency (a.) (in %-points) and the overall losses (b.) (in %)

Table 3: Average measured power losses ($500 \leq n \leq 3000$ rpm, $100 \leq p_2 \leq 400$ bar)

	without shuttles	with shuttles	reduction	
overall power loss [kW]	1,93	1,14	0,79 kW	41,0%
hydromechanical power loss [kW]	1,60	0,99	0,60 kW	37,9%
volumetric power loss [kW]	0,33	0,15	0,19 kW	55,9%

The most remarkable results are at operating speeds below 1000 rpm. In this area, the overall efficiency has been increased by more than 30%-points. For instance at 100 rpm and 400 bar, the shuttles have increased the overall efficiency from a value of 49,6% to 75,3%, an increase of 33,5%-points.

Table 3 shows the split of the total power losses in hydromechanical power losses and volumetric power losses. As before, the data are average values of all test points between $500 \leq n \leq 3000$ rpm and $100 \leq p_2 \leq 400$ bar. The losses are defined according to [18].

The measurements show that the largest improvement of the overall power losses comes from the reduced hydromechanical losses. From the 0,79 kW reduction of total power losses, 0,60 kW is caused by the reduction of the hydromechanical losses. The rest (0,19 kW) originates from the reduced volumetric losses. The next two paragraphs will look in more detail into the hydromechanical and volumetric losses.

4.2. Reduced torque and hydromechanical losses

Figure 5a shows the relative reduction of the hydromechanical part of the power losses, defined as follows:

$$\frac{(P_{loss,hm,without} - P_{loss,hm,with})}{P_{loss,tot,without}} \quad (2)$$

For comparison, figure 5b plots once more the measured reduction of the total power losses with respect to the overall power losses when no shuttles are applied. This is the same diagram as shown in Figure 4b.

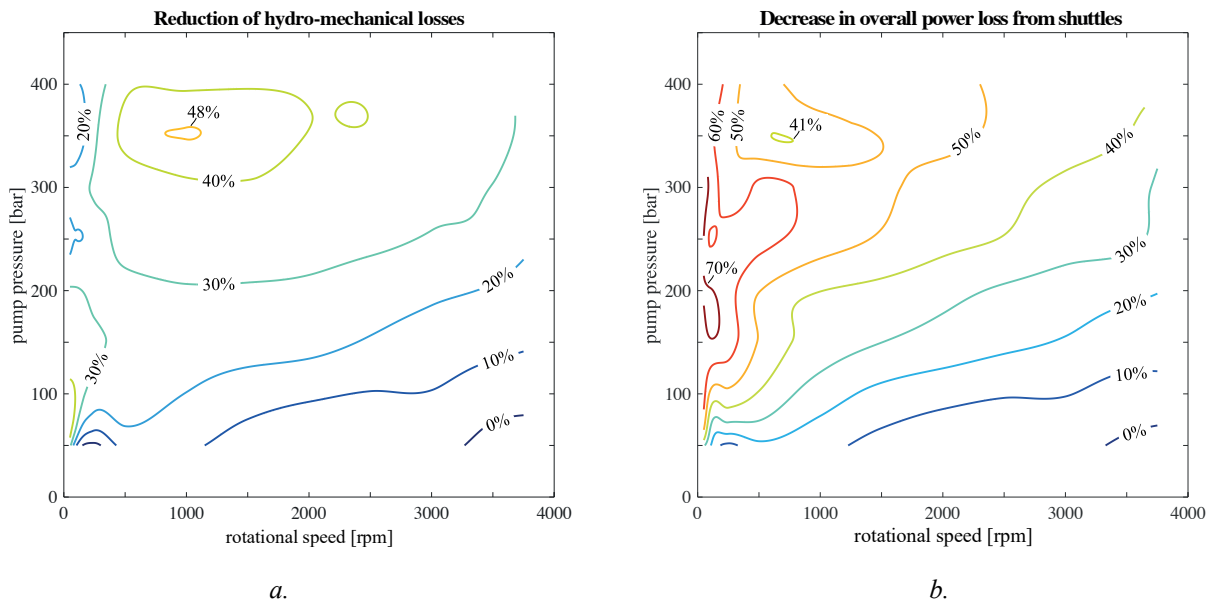


Fig. 5: Reduction of the hydromechanical power losses (a.) and reduction of the overall power losses (b.) relative to the overall power losses when no shuttles are applied

The diagrams of Figure 5 show that the reduction of the overall power loss is dominated by a reduction of the hydro-mechanical losses. At 1000 rpm and 300 bar, the reduction of the hydro-mechanical losses is larger than the decrease of the overall power loss. This is due to an increase of the volumetric losses in this point, which will be discussed later.

It could be possible that the shuttles affect the geometrical displacement of the pump, and thus reduce the driving torque. However, for both pumps, the method of Toet [21] resulted in the same geometrical displacement volume (27,9 cc). The shuttles therefore do not influence the pump capacity, which allows for a direct comparison of the driving torque of the two pumps.

Figure 6 shows the measured difference in required torque input at various operating conditions. The relatively modest reduction of the drive torque at rotational speeds above 1000 rpm was expected due to the elimination of the commutation losses. In this area, the reduction, or even elimination, of the commutation losses results in an efficiency improvement of 3% on average.

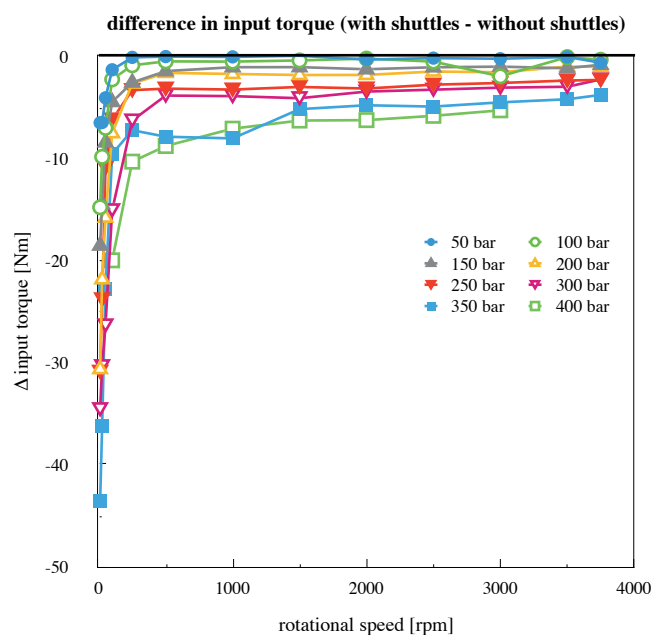


Fig. 6: Reduction of the input torque as a result of applying shuttles in the A4FO28

In the area below 1000 rpm, the overall efficiency is, on average, improved by more than 10%-points, from 79,0% to 89,5%. Figure 7 compares, at a pump pressure of 350 bar, the measured input torque, with and without shuttles. At the lowest speed measured (10 rpm), the input torque was reduced by as much as 20% or 44 Nm. Apparently, the shuttles not only reduce the commutation losses, but also result in a reduction of the friction of the pump itself, in particular of the mixed and solid friction at low speed conditions.

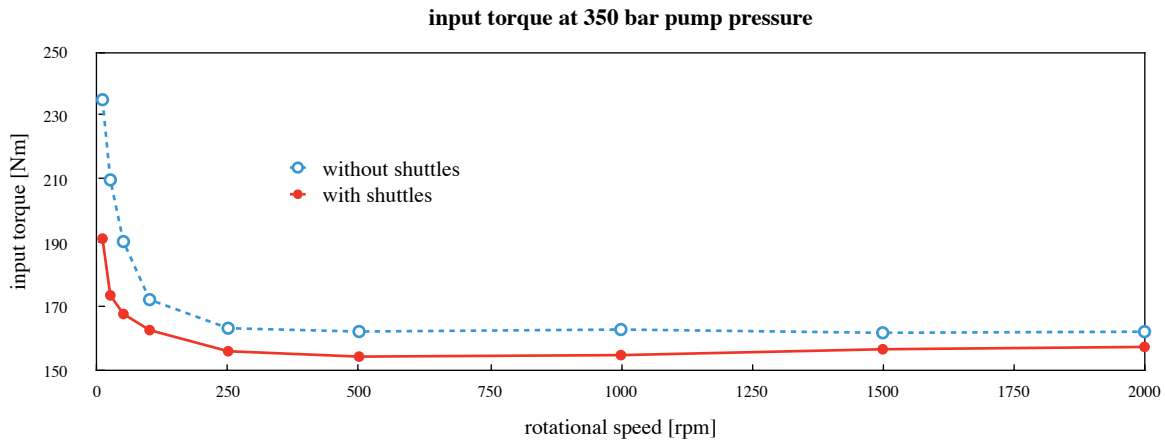


Fig. 7: Measured input torque at a pump pressure of 350 bar

4.3. Reduced volumetric losses

The use of shuttles has also influenced the volumetric losses of the pump. Figure 8a shows the reduction of the volumetric power losses, divided by the overall power loss of the pump without shuttles applied:

$$\frac{(P_{loss,vol,without} - P_{loss,vol,with})}{P_{loss,tot,without}} \quad (3)$$

As before, the relative reduction of the overall power losses is shown in Fig. 8b for comparison. Almost in all operating points, the shuttles have resulted in a reduction of the volumetric losses. Only at 1000 rpm and 350 bar an increase of the volumetric power loss was measured. In all other points, the volumetric losses of the pump were reduced by the shuttles, especially at low rotational speeds.

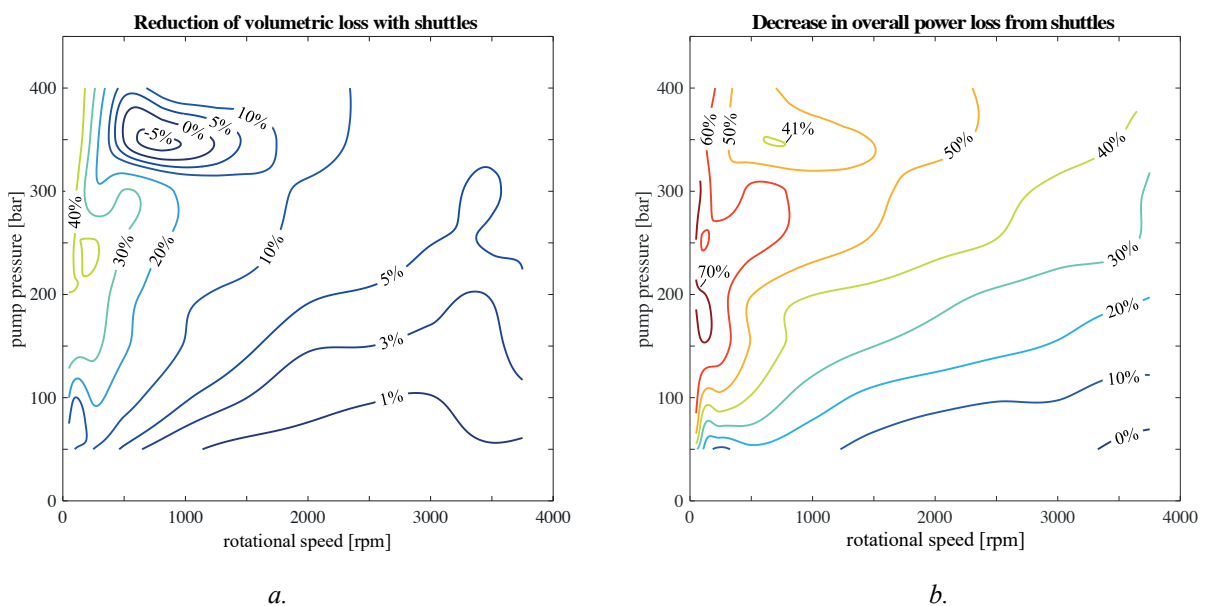


Fig. 8: Reduction of the volumetric power losses (a.) and the overall power losses (b.) relative to the overall power losses when no shuttles are applied

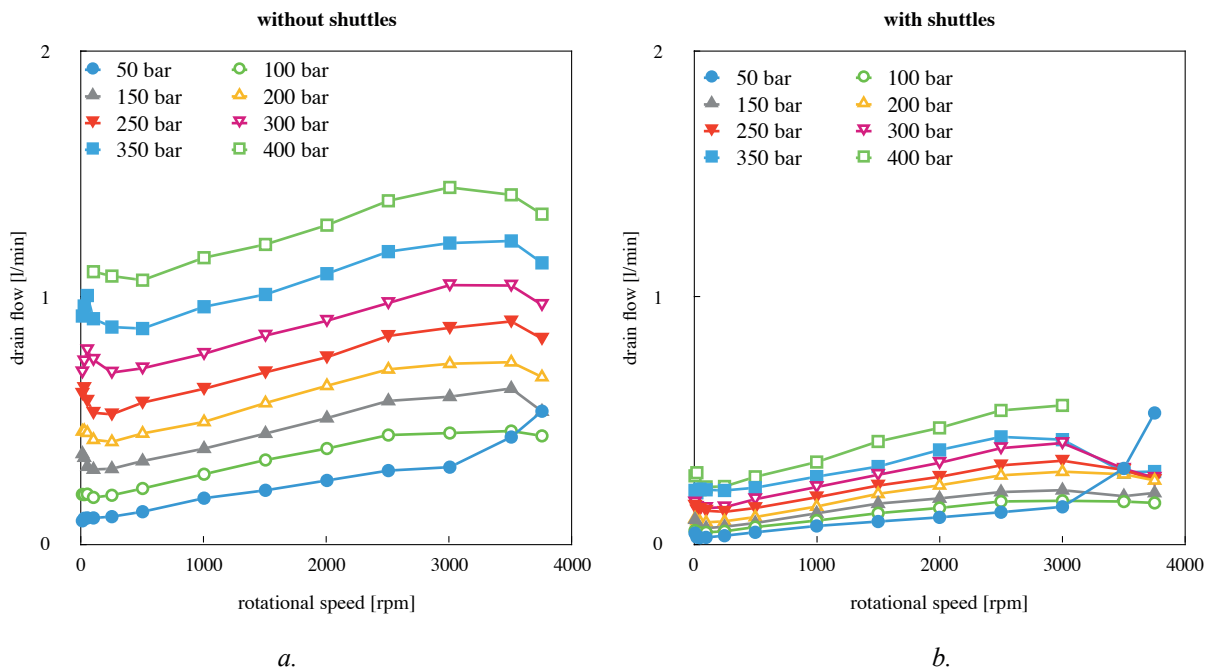


Fig. 9: Measured drain flow from the pump without (a.) and with (b.) shuttles applied

The volumetric losses can be divided in losses which are directly flowing and leaking between the high and low pressure side of the pump (i.e. cross-port leakage), and losses which directly leak to the housing. These last leakage drain losses are measured for both pumps. The results are shown in the two diagrams of Figure 9. By applying shuttles, the drain leakage has been reduced by about 70%.

5. Conclusions

A 28 cc conventional slipper type pump (A4FO28 from Bosch Rexroth) fixed displacement axial piston pumps has been converted to allow shuttles to be applied. In a field of 104 points, stationary performance measurements have been performed. First with the original pump, without the shuttles. After this test, shuttles were mounted in the cylinder block or barrel and the valve plate was replaced by a new design to be combined with the shuttle operation. Finally, the same performance test was performed with the converted pump. The objective of the tests was to measure the effects of the shuttles on the overall efficiency, the overall losses, the hydromechanical and volumetric losses and the drain leakage in a wide range of operating points.

The experiments have proven the shuttles substantially increase the overall efficiency. The total losses are reduced by 41% on average, and up to 60% at high pump pressure and low rotational speeds.

Table 4: Overall efficiencies and total power loss

	without shuttles	with shuttles	effect of the shuttles
average efficiency ($500 \leq n \leq 3000, 100 \leq p_2 \leq 400$)	90,8%	94,3%	+ 3,5%-points
peak efficiency	91,9%	96,4%	+ 4,5%-points
average overall power loss ($500 \leq n \leq 3000, 100 \leq p_2 \leq 400$)	1,93 kW	1,14 kW	-0.79 kW (-41%)

The improvement is largely due to a reduction of the hydromechanical losses. Part of the improvement is a result of a reduction of the commutation losses, which was the reason for developing the shuttle-solution. But the

measurements show that, on top of the reduced commutation losses, the shuttles also reduce friction losses in the pump itself, especially at low rotational speeds. The shuttles also reduce the volumetric power losses by 56% and the drain leakage by about 70% on average. The reduction of the volumetric loss is most probably partly due to the elimination of the silencing grooves, i.e. of the negative overlap which exists in the original port plate.

It should be noted that this is the first test result of shuttles in a conventional pump. It is expected that the shuttles can be improved even further when the design of the shuttles is integrated in the design of a new pump, instead of adapting a conventional pump.

According to the design principle, the shuttles also work in hydrostatic motors, and in two-quadrant pump/motors. In theory, the shuttles might also work in variable displacement machines. In these pumps and motors, the detrimental effects of the dead volume is much more important than in fixed displacement machines. It is therefore expected that the shuttles could even result in higher efficiency improvements than in fixed displacement machines. Further development work and experiments are needed in this direction.

Nomenclature

<i>Variable</i>	<i>Description</i>	<i>Unit</i>
n	rotational speed	[rpm]
p_2	pump pressure	[bar]
P_{loss}	Power loss	[kW]

<i>index</i>	<i>Description</i>
<i>tot</i>	total or overall
<i>hm</i>	hydromechanical
<i>vol</i>	volumetric
<i>without</i>	without shuttles applied
<i>with</i>	with shuttles applied

References

1. Mommers, R., et al, *Commutation Loss in Hydrostatic Pumps and Motors*, Proc. ASME/BATH 2021 Symposium on Fluid Power and Motion Control, 2021, <https://doi.org/10.1115/FPMC2021-68277>
2. Achten, P., et al, *'Shuttle' technology for noise reduction and efficiency improvement of hydrostatic machines*, The Seventh Scandinavian International Conference on Fluid Power, SICFP'01, part 3, page 269, ISBN 91-7383-056-4, 2001
3. Mommers, R. and Achten, P., *'Shuttle' Technology for Noise Reduction and Efficiency Improvement of Hydrostatic Machines - Part 2*, Proc. ASME/BATH 2021 Symposium on Fluid Power and Motion Control, 2021, <https://doi.org/10.1115/FPMC2021-67874>
4. Kuipers, G., *Kompressionsverluste in Axialkolbenpumpen*, Ölhydraulik und Pneumatik 17 (1973) Nr. 8, p. 221-224
5. Douma, O. and Ottens, E., *Kompressionsverluste in Axialkolbenpumpen*, Ölhydraulik und Pneumatik 19 (1975) Nr. 6, p. 469-473
6. Xu, B., et al. *Effects of the dimensional and geometrical errors on the cylinder block tilt of a high-speed EHA pump*. Meccanica 52, 2449–2469 (2017). <https://doi.org/10.1007/s11012-016-0590-0>
7. Wilhelm, S. R., and Van de Ven, J. D. *Design and Testing of an Adjustable Linkage for a Variable Displacement Pump*. ASME. J. Mechanisms Robotics. November 2013; 5(4): 041008. <https://doi.org/10.1115/1.4025122>
8. Wilhelm, S., and Van de Ven, J. *Adjustable Linkage Pump: Efficiency Modeling and Experimental Validation*. ASME. J. Mechanisms Robotics. August 2015; 7(3): 031013. <https://doi.org/10.1115/1.4028293>
9. Göllner, W., Rahmfeld, R. and Hames, B, *The Design of Powersplit Transmissions Using New Technologies of Hydrostatic Components*, Proc. of the ASME/Bath 2017 Symposium on Fluid Power and Motion Control, FPMC2017, October 16-19, 2017, Sarasota, Florida, USA, Paper nr. FPMC2017-4299, <https://doi.org/10.1115/FPMC2017-4299>
10. Pettersson, M., Weddfelt, K., Palmberg, J.-O., *Methods of Reducing Flow Ripple from Fluid Power Pumps - a Theoretical Approach*, Proc. SAE International Off-Highway & Powerplant Congress & Exposition, 1991, SAE Technical Paper 911762, <https://doi.org/10.4271/911762>

11. Kumar Seeniraj, G., M. Zhao, and M. Ivantysynova, *Effect of Combining Precompression Grooves, PCFV And DCFV on Pump Noise Generation*. International Journal of Fluid Power, 2011. 12(3): p. 53-63, <https://doi.org/10.1080/14399776.2011.10781037>
12. Helgestad, B.O., K. Foster, and F.K. Bannister, *Pressure Transients in an Axial Piston Hydraulic Pump*, Proc. of the Institution of Mechanical Engineers, 1974. 188(1): p. 189-199, https://journals.sagepub.com/doi/abs/10.1243/PIME_PROC_1974_188_021_02
13. Harrison, K.A. and K.A. Edge, *Reduction of axial piston pump pressure ripple*. Proc. of the Institution of Mechanical Engineers, Part I: Journal of Systems and Control Engineering, 2000. 214(1): p. 53-64, <https://journals.sagepub.com/doi/abs/10.1243/0959651001540519>
14. Johansson, A., *Design principles for noise reduction in hydraulic piston pumps : simulation, optimisation and experimental verification*, Linköping Studies in Science and Technology. Dissertations. 2005, Linköpings universitet: Linköping, <http://urn.kb.se/resolve?urn=urn:nbn:se:liu:diva-31420>
15. Johansson, A., J. Övander, and J.-O. Palmberg, *Experimental verification of cross-angle for noise reduction in hydraulic piston pumps*. Proc. of the Institution of Mechanical Engineers, Part I: Journal of Systems and Control Engineering, 2007. 221(3): p. 321-330, <https://journals.sagepub.com/doi/abs/10.1243/09596518JSCE208>
16. Cho, J., et al. Dynamic Modeling of an Indexing Valve Plate Pump. in ASME 1999 International Mechanical Engineering Congress and Exposition. 1999, <https://doi.org/10.1115/IMECE1999-0764>
17. Achten, P., Potma, J., and Eggenkamp, S., *A new hydraulic pump and motor test bench for extremely low operating speeds*. Proc. ASME/BATH 2017 Symposium on Fluid Power and Motion Control,, October 16–19, 2017, <https://doi.org/10.1115/FPMC2017-4232>
18. Achten, P., et al, *Measuring the Losses of Hydrostatic Pumps and Motors: A Critical Review of ISO4409:2007*, Proc. ASME. FPMC2019, ASME/BATH 2019 Symposium on Fluid Power and Motion Control, V001T01A007, October 7–9, 2019, <https://doi.org/10.1115/FPMC2019-1615>
19. Bosch Rexroth, *Axial piston fixed pump A4FO re91455_2015-03*, 2015
20. INNAS, *Performance of hydrostatic machines - Extensive measurement report*. 2020, INNAS, Breda, the Netherlands, <https://www.innas.com/assets/performance-of-hydrostatic-machines.pdf>
21. Toet, G., et al., *The Determination of the Theoretical Stroke Volume of Hydrostatic Positive Displacement Pumps and Motors from Volumetric Measurements*. Energies 2019, 12, 415. <https://doi.org/10.3390/en12030415>

Appendix A: Sensor Information

Table A.1: List of sensors in the test bench and their specifications.

Variable	Symbol	Sensor	Range	Accuracy	resolution
Torque	T	Kistler 4541A / 4550A500	-500...500 Nm	±0,25 Nm	
Supply pressures	p ₁	Honeywell TJE 500 psig	0...34.5 bar	±0,035 bar	
Discharge pressure	p ₂	Honeywell STJE 7500 psig	0...517.1 bar	±0,259 bar	
case pressure	p ₃	Omega DYM02MDD0-040BARCV	0...40 bar	±0,02 bar	
Flow rate	Q ₂	VSE RS 400/32	1.0...400 l/ min	0.5% MV*	
Leakage flow	Q ₃	VSE VSI 0.1/16	0.01...10 l/ min	0.3% MV*	
Temperature	t ₁ , t ₂ , t ₃	Testo type 13 PT100 class B	-50...+400 °C	±0.3 °C	
rotational speed	n	Kistler 4541A / 4550A500			60 pulses/rev

*accuracy for this sensor is defined as a percentage of the measured value (MV)

Appendix B: Measured values of the overall efficiency

The following two tables show the measured values of the overall efficiency of the A4FO28

Table B1: Without shuttles

rotational speed [rpm]	pump pressure p_2 [bar]							
	50	100	150	200	250	300	350	400
10								
25	0,544							
50	0,713	0,691	0,646	0,524	0,456	0,318		
100	0,825	0,835	0,806	0,736	0,724	0,623	0,571	0,496
250	0,892	0,907	0,896	0,881	0,866	0,840	0,825	0,772
500	0,890	0,918	0,919	0,912	0,903	0,894	0,886	0,860
1000	0,880	0,914	0,918	0,919	0,914	0,911	0,901	0,890
1500	0,860	0,907	0,916	0,919	0,916	0,915	0,909	0,902
2000	0,843	0,899	0,912	0,919	0,918	0,917	0,912	0,906
2500	0,826	0,890	0,907	0,916	0,916	0,917	0,914	0,910
3000	0,812	0,881	0,902	0,913	0,915	0,917	0,914	0,911
3500	0,795	0,871	0,896	0,908	0,911	0,914	0,913	0,911
3750	0,787	0,867	0,891	0,902	0,905	0,903	0,900	0,895

Table B2: With shuttles

rotational speed [rpm]	pump pressure p_2 [bar]							
	50	100	150	200	250	300	350	400
10								
25	0,779	0,811	0,783					
50	0,828	0,872	0,869	0,837	0,799	0,805	0,746	0,753
100	0,887	0,913	0,935	0,913	0,881	0,869	0,834	0,831
250	0,910	0,950	0,961	0,956	0,951	0,922	0,906	0,896
500	0,917	0,946	0,958	0,956	0,964	0,958	0,927	0,920
1000	0,893	0,930	0,946	0,951	0,960	0,960	0,940	0,951
1500	0,872	0,919	0,940	0,948	0,956	0,958	0,953	0,955
2000	0,854	0,910	0,934	0,944	0,952	0,954	0,957	0,954
2500	0,837	0,899	0,927	0,939	0,948	0,951	0,954	0,952
3000	0,819	0,888	0,920	0,934	0,943	0,947	0,950	0,949
3500	0,796	0,878	0,911	0,927	0,939	0,943	0,947	
3750	0,781	0,873	0,907	0,921	0,930	0,930	0,932	